CCFE
CULHAM CENTRE FOR FUSION ENERGY

UK Atomic Energy Authority

UKAEA-CCFE-PR(23)165

K. Kirov, C. Challis, E. De la Luna, J. Eriksson, D. Gallart, J. Garcia, M. Gorelenkova, J. Hobirk, P. Jacquet, A. Kappatou, Y. Kazakov, D. Keeling, D. King, E. Lerche, C. Maggi, J. Mailloux, P. Mantica, M. Mantsinen, M. Maslov, S. Menmuir, P. Siren, Z. Stancar, D. Van Eester, JET Contributors

Impact of RF waves – fast NBI ions interaction on the fusion performance in JET DTE2 campaign

Impact of RF waves – fast NBI ions interaction on the fusion performance in JET DTE2 campaign

K. Kirov, C. Challis, E. De la Luna, J. Eriksson, D. Gallart, J. Garcia, M. Gorelenkova, J. Hobirk, P. Jacquet, A. Kappatou, Y. Kazakov, D. Keeling, D. King, E. Lerche, C. Maggi, J. Mailloux, P. Mantica, M. Mantsinen, M. Maslov, S. Menmuir, P. Siren, Z. Stancar, D. Van Eester, JET Contributors

This is a preprint of a paper submitted for publication in Nuclear Fusion

Impact of RF waves – fast NBI ions interaction on the fusion performance in JET DTE2 campaign

K. K. Kirov[1, a)], C. D. Challis[1], E. De la Luna[2], J. Eriksson[3], D. Gallart[4], J. Garcia[5], M. Gorelenkova[6], J. Hobirk[7], P. Jacquet[1], A. Kappatou[7], Ye. O. Kazakov[8], D. Keeling[1], D. King[1], E. Lerche[1,8], C. Maggi[1], J. Mailloux[1], P. Mantica[9], M. Mantsinen[4,10], M. Maslov[1], S. Menmuir[1], P. Siren[1], Z. Stancar[1], D. Van Eester[8] and JET Contributors*
EUROfusion Consortium, JET, Culham Science Centre, Abingdon, OX14 3DB, UK

[1] *United Kingdom Atomic Energy Authority, Culham Science Centre, Abingdon OX14 3DB, United Kingdom*
[2] *Laboratorio Nacional de Fusión, CIEMAT, 28040 Madrid, Spain*
[3] *Department of Physics and Astronomy, Uppsala University, SE-75120 Uppsala, Sweden*
[4] *Barcelona Supercomputing Center, Barcelona, Spain*
[5] *CEA, IRFM, F-13108 St-Paul-Lez-Durance, France*
[6] *PPPL, Princeton University, P.O. Box 451, Princeton NJ 08543-0451, USA*
[7] *Max-Planck-Institut für Plasmaphysik, Boltzmannstr. 2, 85748 Garching, Germany*
[8] *Laboratory for Plasma Physics, ERM/KMS, B-1000 Brussels, Belgium*
[9] *Institute of Plasma Science and Technology, CNR, 20125 Milano, Italy*
[10] *ICREA, Barcelona, Spain*
* *See the author list of 'Overview of JET results for optimising ITER operation' by J. Mailloux et al 2022 Nucl. Fusion 62 042026*

[a)] *Corresponding author:* Krassimir.Kirov@ukaea.uk

Abstract. This work studies the interaction between Radio Frequency (RF) waves used for Ion Cyclotron Resonance Heating (ICRH) and the fast Deuterium (D) and Tritium (T) Neutral Beam Injected (NBI) ions in DT plasma. The focus is on the effect of this interaction, also referred to as synergistic effects, on the fusion performance in the recent JET DTE2 campaign. Experimental data from relevant diagnostics were analyzed and conclusions were drawn and supported by modelling of the synergistic effects. TRANSP runs with and without RF kick operator predicted moderate increase, about 10%, in DT rates for the case of RF wave - fast D NBI ions interactions at n=2 harmonic of ion cyclotron resonance and negligible impact by synergistic interaction between fast T NBI ions and RF waves. JETTO modelling gives 29% enhancement of fusion rates due to RF waves – fast D NBI ions interaction and 18% enhancement for fast T NBI ions. Analysis of experimental neutron rates compared to TRANSP predictions without synergistic effects and Magnetic Proton Recoil (MPRu) neutron spectrometer indicate approximately 25-28% enhancement of fusion rates due to RF interaction with fast D ions and approximately 5-8% when RF wave – fast T NBI ions interaction is taking place. Contribution of various heating and fast ion sources have been assessed and discussed.

INTRODUCTION

Plasma heating by means of Radio Frequency (RF) waves in Ion Cyclotron Resonance Heating (ICRH) range of frequencies is widely used in present tokamaks [1]. It is also one of the main heating sources that will be used in devices planned for the near future, including the ones which have been foreseen to operate in Deuterium Tritium (DT) mixture [2], [3]. The presence of DT mixture in burning fusion plasma largely determines the heating scenario to be used with RF waves.

Several ICRH schemes in DT plasma are proposed [2], [4], [5], [6] for the ITER reactor [7], [8]. Well established H minority heating scenario at fundamental frequency in D plasmas is not considered for ITER due to available frequency ranges and partially due to the anticipated parasitic interaction of the RF waves with energetic alphas. The most viable scheme considered for ITER during the active DT phase is by means of ICRH heating of minority ^{3}He at fundamental frequency. In conditions of central toroidal magnetic field of 5.2T and RF waves at 52.5MHz and parallel refractive index of $N_{||}\approx 27$, i.e. ITER's ^{3}He minority heating scenario [2], [4], alphas and fast D ions will interact with RF waves at n=1 resonance at major radius shifted from the plasma center by $R\text{-}R_0\approx$-1.6 m [9]. Fast ions with Doppler shift corresponding to parallel velocities of about $v_{||}\approx 1\times 10^7$ m/s will have more central resonance. In particular, 0.8-1MeV negative NBI D ions can also have required Doppler shift of $v_{||}\approx 1\times 10^7$ m/s.

It is widely acknowledged that in conditions of burning DT plasmas energetic alphas as well as both reactants, D and T ions, can also absorb RF power at fundamental n=1 [4], [9], [10] or harmonic n=2 frequency [11]. This phenomena is also called synergistic effects and it has been reported in numerous studies [11], [12], [13], [14], [15], [16], [17], [18], [19], [20], [21]. In case of H or ^{3}He minority heating schemes, reactants D and T ions are required to have certain energy in order to satisfy Doppler shifted resonance condition necessary for good absorption [12]. Understanding the interaction between RF waves and fast ions is essential in order to (a) understand if there is a benefit on the fusion performance from heating directly fusion reactants, fast D and T ions, via RF waves; (b) study the impact of interaction of RF waves with fast ions on heating, i.e. do the accelerated fast ions or alphas have different heating efficiency and (c) to assess the impact of ICRH heating on energetic particles with regard to orbit losses.

This paper discusses the synergy between RF waves at frequency close to n=2 D and n=2 T resonances and energetic D and T ions generated by Neutral Beam Injection (NBI) in JET. Data from the recent JET DT experimental campaign (DTE2) were analyzed. NBI which was the source of fast D and T populations and ICRH were the only auxiliary heating sources in the experiments discussed here.

When plasma is predominantly heated by NBI, there are in general two contributions to the fusion rates: thermal and Beam-Target (BT) reactions. In typical JET conditions, i.e. ion temperature $T_i\approx$10keV and NBI power $P_{NBI}\approx$25-30MW, thermal and BT rates are of similar magnitude for DT mixture with nearly equal D and T densities. There are also Beam-Beam (BB) reactions, but they are at least two orders of magnitude lower than BT rates and therefore their contribution is usually ignored. The thermal DT reactivity $\langle\sigma.v\rangle$ peaks up for ion temperatures of DT mixture at about $T_i\approx$65keV, while BT reactions have different maxima for fast D/T collisions on thermal T/D ions. In conditions of JET DT plasma, the latter are for energies of $E_D\approx$127keV and $E_T\approx$192keV, figure 1. In general, the JET NBI system can inject fast D and T ions with maximum energy of the order of $E_{full}\approx$110-120keV. A substantial amount of the fast ions is however born with energies between half, $E_{full}/2$, and a third, $E_{full}/3$, of this energy as shown by shaded rectangle at the bottom left on figure 1. At these energy levels BT reactions are not fully optimized for fusion performance and further energizing of fast NBI D and T ions would have a beneficial impact on BT rates. Although NBI D ions full energy is of the order of $E_{full}\approx$ 120keV, i. e. close to the maximum of BTDT, the bulk of fast ions produced by NBI is for lower energies: approximately 46% of NBI fast ions are born at $E_{full}/2$, and about 21% at $E_{full}/3$. Therefore, accelerating lower energy fast D ions in the range between $E_{full}/2$ and $E_{full}/2$ will be obviously beneficial regarding BT rates. As for the fast T NBI ions, the gap between JETs NBI capabilities and BT maximum is larger and accelerating them up to 200keV can be regarded as greatly beneficial, figure 1.

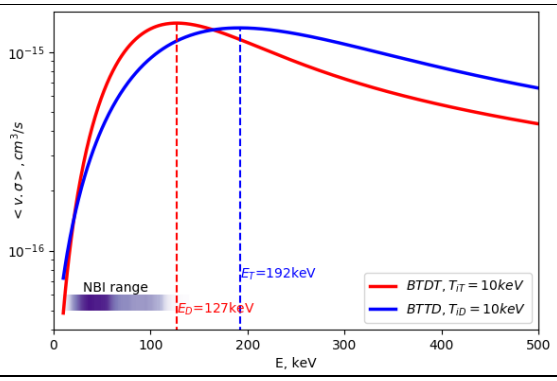

FIGURE 1. Beam-Target reactivities $\langle\sigma.v\rangle$ for DT reaction of a mono energetic beam with energy E on target ions with temperature of T_i=10keV. D beams on T target ions reactivity (red) is noted by BTDT, while T beam on D target ions reactivity (blue) is noted by BTTD. The maximum of the two reactivities is noted by vertical dashed lines, $\langle\sigma.v\rangle$ = 1.40×10^{-15}cm^3/s at E_D=127keV for BTDT and $\langle\sigma.v\rangle$ = 1.32×10^{-15}cm^3/s at E_T=192keV for BTTD. The energy range of JET NBI source approximately noted by a horizontal shaded area color coded by fast ion density at the bottom left corner.

It is well known from the literature [22] that for the fast ions the critical energy and the electron-ion slowing down time determine their dynamics in hot plasma. An estimate of these parameters is provided here for DT=0.5/0.5 mixture at T_e=10keV, $n_e=7\times10^{19}$ m^{-3}, table 1. Estimates are based [23], [24] on the following well known expressions:

$$W_{crit}[\mathrm{eV}] = 14.8\, T_e[\mathrm{eV}] \left(\frac{A^{3/2}}{n_e} \sum_j \left(\frac{n_j Z_j^2}{A_j}\right)\right)^{2/3} \quad (1)$$

$$\tau_s[\mathrm{s}] = 6.27\times10^{14} \frac{A\, T_e[\mathrm{eV}]^{3/2}}{n_e[\mathrm{m}^{-3}]\, Z^2\, \ln\Lambda} \quad (2)$$

$$\tau_{th}[\mathrm{s}] = \frac{\tau_s}{3} \ln\left[1 + \left(\frac{W}{W_{crit}}\right)^{3/2}\right] \quad (3)$$

Where A is fast ion atomic mass, A_j and Z_j are plasma composition atomic mass and charge, n_j is plasma ion density, $\ln\Lambda$ is the Coulomb logarithm, W_{crit} is ions critical energy, τ_s is the electron-ion slowing down time and τ_{th} is the thermalization time for typical energies of the fast ions.

TABLE 1. Typical parameters for various fast ions in fusion plasma at D/T=0.5/0.5 plasma mixture and T_e=10keV, $n_e=7\times10^{19}$ m^{-3}. Critical energy, eq. (1), electron-ion slowing down time, eq. (2), and thermalization time, eq. (3), are calculated for ions typical anergy <W>. In these estimates $\ln\Lambda$ = 17 was assumed.

Fast ion specie,	typical energy, <W>, keV	Critical energy, W_{crit}, keV	Electron-ion slowing down time, τ_s, s	Thermalization time, τ_{th}, s
NBI D,	Injected at ~100keV (acc. to 400keV)	165keV	1.05s	0.14s (0.55s)
NBI T,	Injected at ~100keV (acc. to 400keV)	248keV	1.58s	0.12s (0.59s)
Minority H,	Accelerated to typical energies of ~200keV	83keV	0.52s	0.27s
Minority ^{3}He,	Accelerated to typical energies of 80keV	248keV	0.39s	0.02s
Fusion alphas,	Born at 3500keV	330keV	0.53s	0.62s

One should note that the estimates in table 1 cover only particular case where plasma parameters, n_e, T_e, A_j and Z_j, are close to the specified ones, ion Larmour radius are small and orbits do not deviate significantly from flux surfaces. In real experiments where plasma parameters, n_e, T_e and plasma composition vary significantly from plasma core to the edge the parameters in table 1 and eqs. (1)-(3) can change significantly. In general, critical energy is linear with electron temperature, T_e, while slowing down time is proportional to $T_e^{3/2}$ and inversely proportional to electron density, n_e. It is essential to also note that in

general the fast ion species summarized in table 1 do not obey Maxwellian distribution. Except for the thermal fusion born alphas fast ions are also not isotropic.

The study presented here focuses on n=2 ICRH heating of fast NBI D and T ions and its impact on the fusion performance. The latter is measured by means of fusion rates which are analogous to neutron rates, both used in total or per unit volume units. Initial assessment of RF wave – fast NBI ions interaction in JET DTE2 experiments was reported in [25]. This report further extends the findings in [25] by means of adding new data and methods of analysis. Section 2 provides details of the numerical tools used in the study. Section 3 presents the experimental conditions and provides details about plasma parameters in the selected JET DT pulses. Section 4 focuses on the analysis of calculated and measured neutron rates. Discussions on the impact of the RF wave – fast ions interaction physics insight of the processes involved is presented in section 5. Summary and conclusions are highlighted in the end.

NUMERICAL TOOLS USED IN THE STUDY

TRANSP [26] code was essentially used for interpretive analysis of the pulses investigated here. In addition, Fast Ion Distribution Functions (FI DF) were calculated by NUBEAM code [27] which is a computationally comprehensive Monte Carlo code for NBI heating in tokamaks. ICRH heating is usually split into two separate modules: RW wave solver, which calculates wave electric field for the target plasma mixture with selected minorities and Fokker–Planck (FP) solver, which provides collisional exchange between heated species and the background plasma. Ideally the two modules, RF wave solver and FP code should be running self-consistently in an iterative loop since changes in heated specie distribution function result in changes in RF wave dispersion and vice versa. In many applications this is, however, a challenging task and achieving convergence between the two solvers might not be possible. In majority of cases of interest, it is sufficiently accurate to assume that only the minority species encounter significant evolution in their distribution function due to power absorption from RF waves and therefore one can use RF wave / FP solver loop for them only. The RF wave solver for TRANSP is TORIC code [28]. It is coupled to a bounce averaging Fokker–Planck solver, FPP code [29], which uses up/down asymmetric equilibria and computes the minority ion phase-space distribution. The energetic minority ion distribution function from FPP is used to compute the collisional transfer of energy to bulk ions and electrons. Energy absorption by electrons, bulk and fast ions can also be assessed in general directly from the wave solver by means of calculating single pass abruption coefficients by each specie from the anti-Hermitian part of dielectric tensor.

To study the RF wave absorption by the fast ions which are treated by NUBEAM code, i.e. NBI ions and alphas, a quasi liner RF kick operator [9] is implemented in NUBEAM [30], [31] and used in this study. TORIC provides information about RF electric field components, E_{+} , E_{-} and $E_{\|}$, and perpendicular wave vector for each toroidal mode. RF resonance condition for a given harmonic is then used to calculate the magnetic moment and energy of the particles satisfying the resonant condition [31]. Every time fast ion passes through resonance layer it receives a kick in magnetic moment space [32]. The magnitude of the kick is derived from the quasi-linear theory [33], while the stochastic nature of the wave-particle interaction is reproduced by means of Monte Carlo random number for the phase of the gyro-orbit.

Additional modelling is performed by means of JETTO code [34] coupled to PION/PENCIL package for computing NBI and RF power absorptions taking into account the synergistic effects. The PION code [35] is used in JETTO for ICRH minority and harmonic heating utilizing its main advantage of being computationally fast thus compatible with integrated modelling. The code interfaces [36] with the existing PENCIL NBI deposition code [37], [38] and accounts for NB and RF synergy effects [36], [13] thus providing flux-surface averaged fast ion distribution function and RF power deposition self-consistently. The orbit effects on fast ions dynamics are neglected in the standalone PENCIL code as the fast ions are constrained to remain on the flux surface of birth throughout the slowing down process. In the PION/PENCIL coupling however, PENCIL only provides fast ion sources to PION, which uses its own slowing down model where orbit effects are included in a simplified way. The effects of toroidal rotation

of the plasma on the BT rates are neglected in PENCIL and this is expected to have a small impact on the calculated neutron rates with rotation velocity in the core estimated to be at approximately 10 times lower than injected beam parallel velocity at maximum energy. In PION/PENCIL package however PION subtracts plasma rotation from beam particle velocity, resulting in up to 5% loss of beam power in strongly rotating plasmas. Recent tests between PION/PENCIL and TRANSP, which takes full account of toroidal rotation effects, were shown to agree within 5% for beam-target DD neutron rates in JET high performance hybrid conditions.

The workflow for the analysis used in this study includes supplying TRANSP and JETTO codes with experimental profiles for electron density, n_e, electron temperature, T_e, ion temperature, T_i, rotation, impurities and effective charge, Z_{eff}. The two codes were then run in interpretative mode which provides deposition profiles by NBI and ICRH heating, fast ion densities and distribution functions and expected neutron rates. The effects of MHD modes on fast ion transport and losses are neglected in this study. In the pulses studied here the q-profile and the start of the heating power were optimized, with $q>1$ for a long enough period after the start of the heating, so that early MHD activities were avoided [39]. Low amplitude and transient n=2, 3 and 4 modes were observed but are thought to be benign with regard to fast ion losses. More central n=1 mode followed by fishbone activities which indicate more intense MHD – fast ions interaction appear much later, t>10s [39], compared to the time slices of interest in our studies.

For the purpose of this study fusion reactions are calculated self-consistently with supplied profiles and calculated fast ion distributions. As discussed in the introduction the two main sources of fusion neutrons, thermal and BT reaction, are approximately of similar order. While thermal neutron rates can be straightforwardly calculated since they are tabulated vs. T_i [40] the calculations of BT rates require detailed knowledge of fast NBI ion DF. The latter is provided by NUBEAM code and the synergistic effects are calculated with the help of RF kick operator. In conditions of JET DTE2 experiments DT fusion reaction has at least two orders of magnitude higher cross-sections than accompanying DD and TT reactions and features distinctive 14.1MeV neutron production. Neutrons created from thermal reactions are nearly monoenergetic and isotropic, while BT neutron spectra can be quite broad and anisotropic [41]. The broadening of spectra of the measured neutrons is directly related to energetic reactants as for instance for BT reactions the higher the energy of fast NBI ions the broader the neutron spectrum is. High energy neutron diagnostics therefore can be used for constraining the interpretative analysis by TRANSP and JETTO. For this purpose, the output of the simulations is used to calculate signals from "synthetic diagnostics" which can then be directly compared with the measurements from the physical diagnostics. Achieving a high level of consistency between measurements and calculations for neutron rates and neutron spectra is an indication of good fidelity of the analysis. The set of available synthetic diagnostics used here includes neutron yield detectors, neutron camera, neutron spectrometers, neutral particle analyzers.

EXPERIMANTAL SET-UP

Diagnostics

Experimental data from standard JET diagnostics were used as input to the simulations discussed in this study. Electron density and temperature profiles were taken from the High Resolution Thomson Scattering diagnostics, referred to as HRTS here. The latter does not cover the very core of the plasma therefore central values on electron density and temperature are taken from LIght Detection And Ranging, LIDAR, measurements [42]. Electron temperature from ECE radiometer [43] was also used in the analysis. Radiated power was measured by the bolometric diagnostics [44], while Z_{eff} was assessed by means of Bremsstrahlung measurements from visible spectroscopy. Ion temperature T_i for the investigated pulses was obtained from Charge eXchange Recombination Spectroscopy (CXRS) diagnostic [45].

With regard to the available synthetic diagnostics a wide range of neutron emission detectors were utilized. Neutron emission diagnostics provide essentially the source of data needed for the purpose of analysis validation. Neutron production counts were taken from the available neutron yield monitors [46].

Details of JET's neutron emission neutron profile monitor are provided in [47]. The instrument comprises two cameras; the horizontal camera consists of 10 collimators for 10 viewing chords and containing detector channels 1-10, views the vertical profile, while the vertical camera, comprising 9 collimators and containing detector channels 11-19, views the horizontal (or radial) profile, figure 2 a).

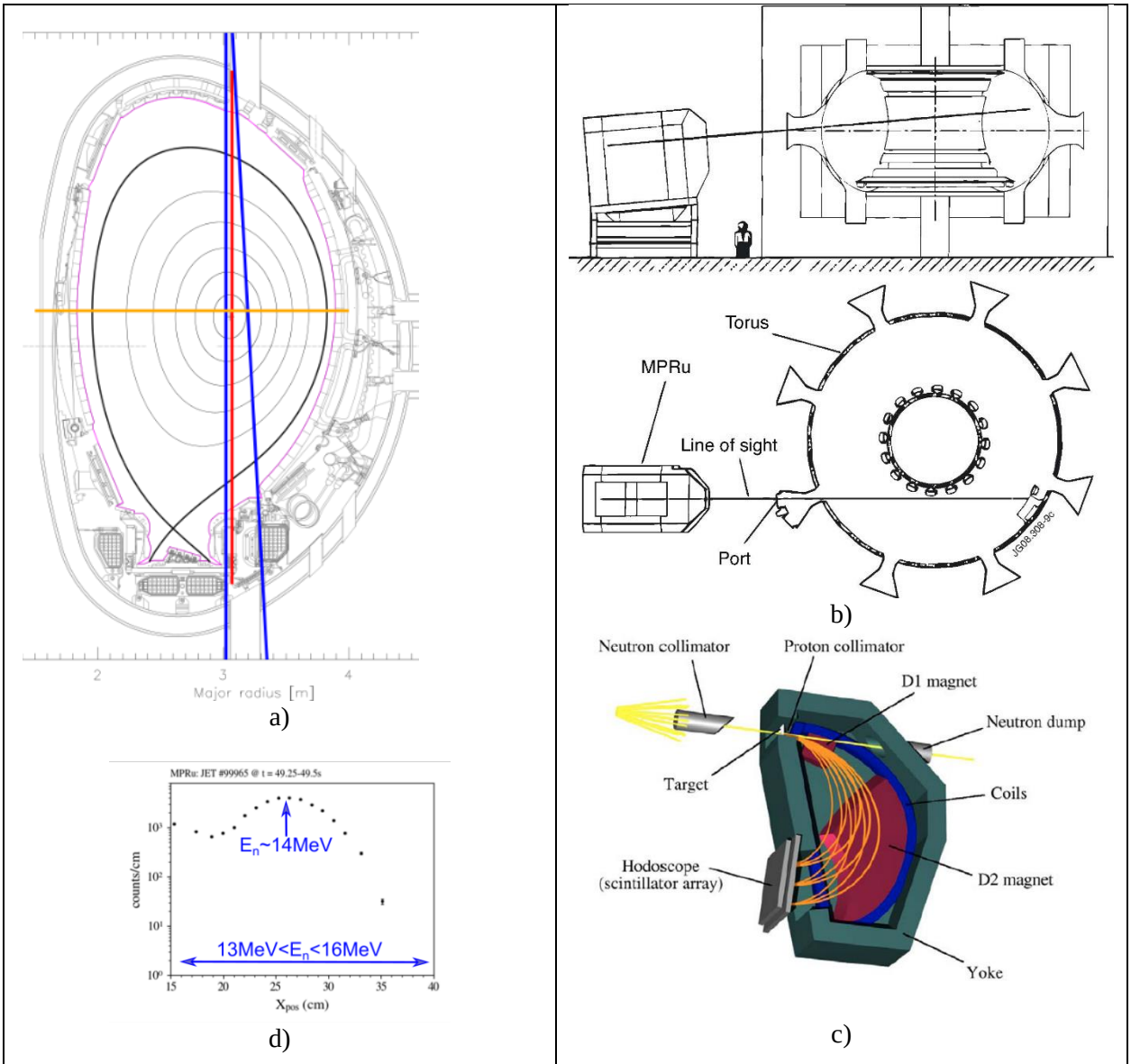

FIGURE 2. Synthetic diagnostics in typical JET configuration for #99643 at 8.5s in a) with Line Of Sight (LOS) of low energy NPA (orange horizontal line), high energy NPA (red vertical line) and central lines of neutron camera (blue lines for channels 15 and 16. Magnetic proton recoil (MPRu) spectrometer schematic is shown in b), while schematic of detector cross-section is in c). The mapping of MPRu scattered proton positions and approximate location of the expected peak at 14MeV are shown in d)

Data from the upgraded Magnetic Proton Recoil (MPRu) spectrometer, figure 2 b), c), were used in the analysis. The upgraded MPRu neutron spectrometer [48], [49] has a horizontal/tangential view of the plasma, figure 2 b), and probes the neutron energy spectrum by letting a collimated beam of neutrons from the plasma impinge on a thin plastic foil, in which some of the neutrons scatter elastically on protons in the

foil, thus producing a secondary beam of protons, with energies that are closely related to the energies of the incoming neutrons. The energy spectrum of the protons is deduced by letting the protons pass through a magnetic field, where they are deflected with different curvature radii depending on their energy. The amount of deflection is determined by recording the strike position, X_{pos}, on an array of scintillator detectors located after the magnetic system, as shown in figure 2 c). Larger values of X_{pos} means a larger radius of curvature and hence a higher energy of the incoming neutron. An example of a measured MPRu spectrum is shown in Figure 2d, together with rough indications of the neutron energies that give rise to the signal in different parts of the spectrum. Precise conversion between X_{pos} and neutron energy is challenging, due to the finite resolution of the spectrometer; however, the resolution function is well known and for a given neutron energy spectrum it is straightforward to determine the expected MPRu spectrum.

Data from JET's neutral particle analyzer [50] was used to provide assessment of the fast ion energies. Neutral particles are detected by means of low energy NPA with horizontal LOS at Z=+0.28m, LOS in figure 2 a) orange line, and high energy NPA, LOS in figure 2 a) red line, which has a vertical LOS at R=3.07m. The former diagnostic is an instrument which has been designed to obtain energy distributions and absolute intensity of hydrogen, deuterium and tritium atoms emitted by fusion plasmas in the total energy range 5 - 740keV for H neutrals, 5 - 370keV for D neutrals, 5 - 250keV for T neutrals. The high energy NPA is capable of time resolved measurements of H, D, T, ^{3}He and ^{4}He atomic flux emitted by the plasma, in the energy range 0.3 - 3.5MeV.

JET DT hybrid pulses

Similar JET 3.43T/2.3MA pulses based on hybrid scenario [39], [51], [52] during DTE2 campaign were selected for the analysis in this study. ICRH was setup as in H or ^{3}He minority heating scenario. Minimum concentration of the minorities was used in some cases to ensure maximum RF power to majority ions, D and T, [53], [54] as minority heating scales with their density. Applied RF power in some cases was modulated with square waveform with 80-90% modulation depth, $P_{ICRH,max}\approx$4-5MW, $P_{ICRH,min}\approx$0.4MW, and low frequency of about 1Hz, which parameters provide sufficiently lengthy time intervals of about 0.5s to be approximated as being with full power ICRH or without ICRH power. In our studies these periods will be also referred to as ICRH power on/off periods. This provides experimental means to assess directly the synergistic effects.

Most of the pulses used in Hybrid scenario used H minority with $X[H]=n_H/n_e\approx$2-3%, while a number of experiments were also performed with ^{3}He minority with $X[^3He]=n_{3He}/n_e\approx$3-4% [53]. There were also pulses without injection of minorities [53], [54], e.g. #99643 was designed to have n=2 D ICRH heating with a frequency of 51.4MHz, while pulses #99884 and #99886 with n=2 T ICRH heating at frequency of 32.2MHz. Although no minorities were injected in these pulses one can assume that there is very small amount of residual H or ^{3}He in the vessel. The supplies of D at JET are usually of high purity, 99.999%, however the data from visible spectroscopy indicate X[H]≈0.2-0.5%, i.e. 2-5 times higher H concentrations, even in the cases where no H was injected. The presence of ^{3}He in the vessel is also difficult to imagine particularly when there were long periods during which ^{3}He was not used. However, bearing in mind that T naturally decays to ^{3}He with half-life of about 12.32 years even the purest T supplies can be easily contaminated with small amount of ^{3}He if they are stored for a longer period.

Plasma parameters and kinetic profiles of #99643 with n=2 D ICRH heating and #99639 with ^{3}He minority, $X[^3He]\approx$3.6%, and n=2 T ICRH heating are shown in figure 3. These two pulses were at similar electron density, line averaged values of about 5×10^{19} m^{-3}, central electron density of about 7×10^{19} m^{-3}, central electron temperature of about 7keV and ion temperature of about 8keV, figure 3 b) and c). Plasma core toroidal rotation of the order of 1×10^5rad/s, i.e. about 3×10^5m/s in the plasma center, was measured during these experiments. Both pulses were analyzed after the transient high-performance phase at the beginning of the heating, i.e. in the period 8.5-9.5s. Analysis during the early phase before 8s is avoided as it does not represent steady state plasma with beams penetrating deeply in the core in conditions with lower

plasma density. Evenly balanced DT mixture, D/T≈0.5/0.5, was sustained in these experiments, while comparable sources of fast D and T ions were provided by the two NBI sources at JET. NBI power between 24 and 30MW was injected by two NBI beamlines, one with D and one with T neutrals. The injected NBI neutrals are at three energy levels, full/half/third energy component with typical values of the power fractions in them 0.5/0.3/0.2 for 100kV of D beam and 0.6/0.2/0.2 for 100kV of T beam. The full energy of the injected D and T neutrals in reported experiments was between 83 and 112kV.

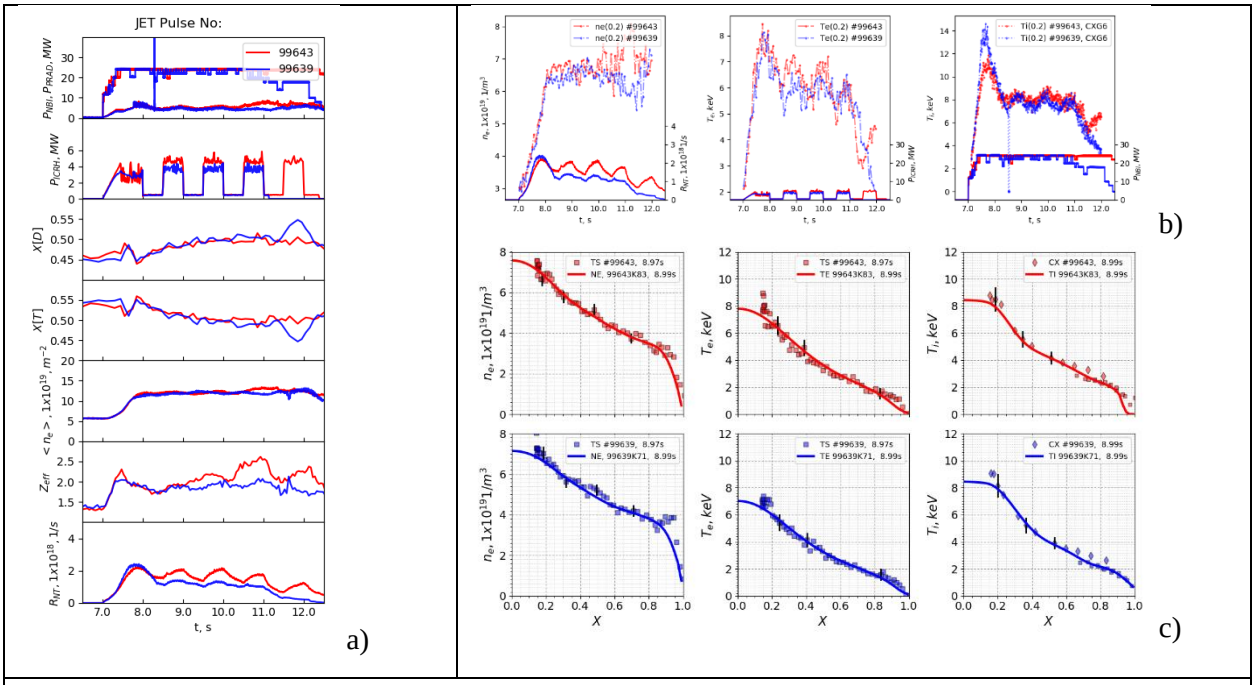

FIGURE 3. a) Time traces of (top to bottom) NBI and radiation power, ICRH power, D concentrations, T concentrations, line integrated density, Z_{eff} and neutron yield for JET 3.43T/2.3MA hybrid type pulses #99643 (red) and #99639 (blue). Time traces from the same two pulses showing (left to right) central density, electron and ion temperature evolution (b). Profiles of electron density, electron and ion temperatures of #99643 (red) and #99639 (blue) at 9s. Measured values are indicted by symbols and error-bars for few radial positions, while smoother profiles used in TARNSP and JETTO interpretative analysis are given by lines.

The other pulses included in analysis and presented here have in general very similar parameters to the ones presented in figure 3. The only differences were in the amount of minorities used in all these pulses. While it is an essential parameter in this study, which determines the amount of RF power available to fast ions, it is worth noting that in many cases, e.g. ^{3}He minority, the minority concentration could not be precisely controlled and kept constant during JET DT pulses.

ANALYSIS OF THE SYNERGISTIC EFFECTS IN RF WAVE FAST NBI IONS INTERACTIONS

Determining the impact of the interactions between the RF waves and fast NBI ions on fusion performance is quite a challenging task. As discussed in the introduction section, the main issues are related to a number of indirect effects of the RF waves on the plasma performance, e.g. providing direct and indirect ion heating, which impacts directly on the fusion performance. Due to the complexity of the problem, for the analysis presented here an approach based on simulations and validation versus available synthetic diagnostics was adopted.

Initially an assessment of the impact of the RF waves - fast NBI ions interaction on the fusion performance was made by performing a pair of TRANSP and JETTO interpretative runs, one with and the other without the effect of RF waves on fast particles. Due to the specifics of both codes this was possible for JETTO modelling by running cases with realistic and negligible RF power, while in TRANSP this was done by switching on and off the RF kick operator. Switching off the RF kick operator in TRANSP will result in discarding the synergistic effects only while all other contributions related to the background plasma parameters will be preserved. As discussed in the experimental section, applied RF power in few cases was modulated with square waveform thus providing sufficiently lengthy time intervals of about 0.5s which can be approximated as being with full power ICRH or without ICRH power. This conclusion is backed up by assessments of the thermalization times shown in table 1 which for both D and T NBI ions with energies of 100keV are much shorter than 0.5s. The thermalization times increase with energy of the fast ions, eq.(3), becoming comparable to 0.5s for fast D and T ions with energies of about 400keV. Based on this estimate, the end of RF power switch off period can be used as a reference to conditions with negligible or no synergistic effects and the RF power switch on period can be used to assess RF waves - fast NBI ions interaction.

In the next section impact of the synergy effects on FI DF is studied first.

Fast ion distribution function

Fast ion density and central distribution function derived by TRANSP for n=2 D pulse #99643 are shown in figure 4 for the cases with RF kick operator and high RF power, figure 4 a) and b), with RF kick operator and low RF power, figure 4 c) and d), and without RF kick operator figure 4 e) and f). High and low RF power phases are here referred to as the periods at the end of modulation phases considered to be approximating steady state with and without synergistic interactions. The high RF power phase during modulation was taken at 8.94s when $P_{RF}\approx$4MW was applied, while lower power phase was selected at 9.44s with $P_{RF}\approx$0.4MW, figure 3 a). Fast D NBI ion density was always peaked in the core, while the cold plasma resonance is also in the vicinity of the mid-radius, figure 4 a). Although negligible minority concentration X[H]=0.5% was assumed in this run, RF wave featured very good first past absorption as shown by the plots of $|E_-/E_+|$ ratio and $|E_+|$ field, figure 5. The graph of the RF E_+ field, figure 5 b), indicate strong $|E_+|$ field in the plasma core facilitating strong absorption by resonant particles.

Central fast D densities were of the order of 5.2×10^{18} m^{-3} for the case with RF kick operator and high RF power, figure 4 a), and 3.8×10^{18} m^{-3} for the case with RF kick operator and low RF power, figure 4 c), and 3.9×10^{18} m^{-3}, for the case without RF kick operator and low RF power, figure 4 e). These numbers are about 5-7% of the central electron density in these pulses, figure 3 b), which is comparable to minorities concentrations used in standard ICRH heating schemes. Fast ion DF and Doppler shifted resonance in figure 4 b) indicate that in the central region (R=3.07m, Z=0.30m) Doppler shift is of the order of $v_{||}\approx1\times10^6$ m/s and there are sufficiently great number of fast D ions with energy of the order of 100keV that can interact with the RF wave. Indeed, because of this interaction fast D ions absorb energy from the RF wave and their DF is modified significantly by pulling a tail for energies above 100keV, figure 4 b). As the injected NBI neutrals were with energies lower than 112kV, the enhancement of fast ions DF for energies higher than 112keV was purely due to interactions between the RF wave and the fast ions. These changes to FI DF have direct and indirect impact on the fusion rates. Direct enhancement of BT rates was a result of increased energy of the fast D ions, i.e. accelerating D ions towards energies of about 130keV has direct impact on BT fusion rates of fast D ions on target T ions, figure 1. The indirect effect of synergistic effects on fusion performance is due to the fact that further energizing the fast D ions leads to enhanced bulk ion heating. The latter is clearly observed from the central T_i modulations with ICRH power in figure 3 b) taking into account negligible minority concentration in this case and assuming bulk D interaction with n=2 RF wave is small. The thermal velocity of bulk D ions, $v_{th,D}=(T_i/m_i)^{1/2}$, is indicated in figure 4 b) by red circle, while the parallel velocity $v_{||}\approx1\times10^6$ m/s needed for Doppler shifted resonance is provided by dashed cyan line.

Only small amount of bulk D ions with small perpendicular velocity $v_\perp$ can interact with RF waves. The intensity of this interaction however is very small as for n=2 it is proportional to combination of Bessel functions, $(J_1(k_\perp v_\perp/\Omega_{ci}) + \lambda J_3(k_\perp v_\perp/\Omega_{ci}))^2$, which is negligible for $v_\perp << 1\times10^6$ m/s [25].

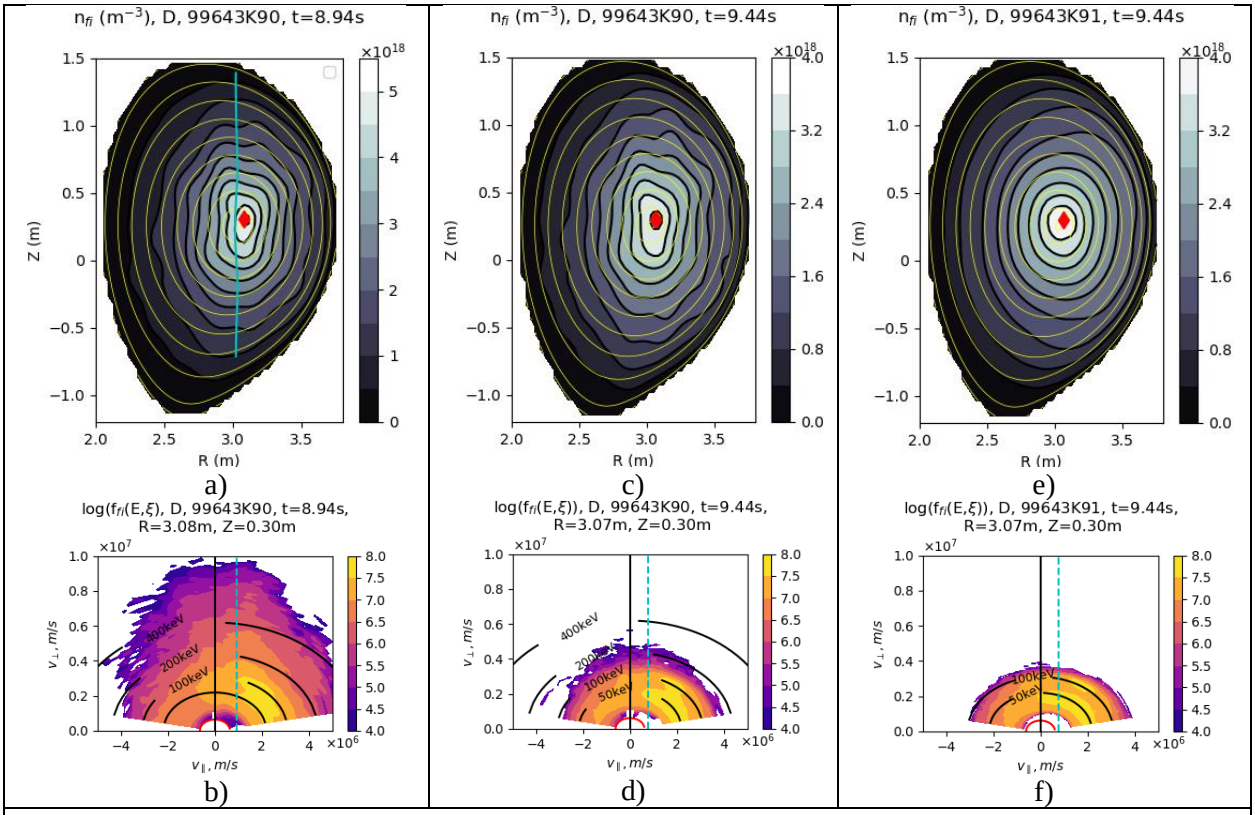

FIGURE 4. Fast D NBI ion density and FI DF from TRANSP code for cases 99643K90 with and 99643K91 without RF kick operator for JET 3.43T/2.3MA hybrid type pulse #99643 with D/T mixture of ≈0.5/0.5. a) Fast D NBI ion density at 8.94s with P_{NBI}≈24MW, P_{RF}≈4MW is shown together with IC n=2 D resonance (cyan line). b) FI DF log($f_{fi}(v_\parallel,v_\perp)$) at 8.94s and R=3.08m, Z=0.30m (point noted with red diamond in a) with FI density of n_{fi}≈5.2×10^{18}m^{-3}) together with Doppler shifted IC resonance (cyan dashed line). c) Same as a) but at 9.44s with P_{NBI}≈22MW, P_{RF}≈0.4MW. d) Fast D NBI ion DF at 9.44s and R=3.07m, Z=0.30m (point noted with red diamond in c) with FI density of n_{fi}≈3.8×10^{18}m^{-3}). e) Same as b) but for case 99643K91, 9.44s without RF kick operator. Unperturbed fast ions DF for case 99643K91, 9.94s without RF kick operator at R=3.07m, Z=0.30m (with FI density of n_{fi}≈3.9×10^{18}m^{-3}) is provided in f).

Fast ion DF with low RF power and with RF kick operator is shown in figure 4 d), while for the case at low RF power and no RF kick it is shown in figure 4 f). Fast ion DF from figure 4 integrated over pitch angle are also shown in figure 6 as function of energy. Comparing figures 4 b), d) and f) one clearly sees the impact of the RF waves on FI DF due to synergistic interactions. Indeed, modified FI DF during high RF power phase of the modulation, figure 4 b) and figure 6 in red, features a significant energetic tail, while FI DF during low RF power phase of the modulation, figure 4 d) and figure 6 in cyan, is essentially relaxed DF and almost does not feature energetic tail. The latter is in fact very similar to the FI DF for the case without RF interaction, figure 4 f) and figure 6 in blue. This observation is used further in this study to support the assumption that fast D ions would slow down to the original unperturbed DF determined by NBI source at the end of low RF power phase, i.e. within ~0.4-0.5s after RF power has become negligible.

The simulations shown in figures 4 b), d) and f) and figure 6 show that in terms of RF waves – fast ions interaction the time at the end of modulation switch off phase is sufficient to allow FI DF to relax to nonperturbed DF. This observation is a basis for a new method of assessment of synergistic effects, which

is not sensitive to RF kick operator implementation. This method is supplementary to the assessment via simulations with and without RF kick operator and it is based on the assumption that TRANSP is able to predict fusion performance with good accuracy. For JET this has been shown in recent DD [55], [56] and DT experiments [57]. Recent reports [58] also highlight that in older JET pulses during JET C wall period neutron rates were largely overpredicted by TRANSP. Since the introduction of JET ILW and improved T_i measurements the statistics show relatively good consistency between measured and calculated neutrons [55], [56], [57].

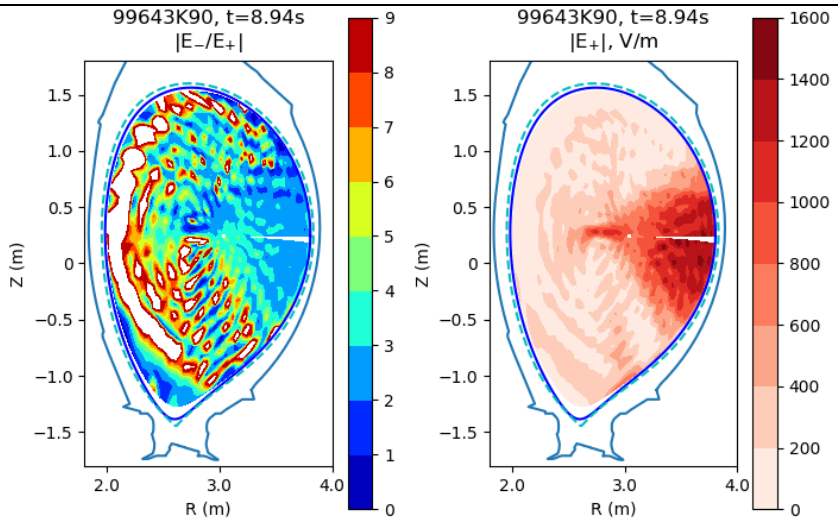

FIGURE 5. Ratio of amplitudes | E_- / E_+ | of E_- and E_+ fields (a) and | E_+ | field in (b) for 3.43T/2.3MA hybrid type pulse #99643 at 8.94s with P_{RF}~4MW by TORIC in conditions with negligible minority H concentrations, X[H]=0.5%

The new method of assessing RF waves – fast ions interaction proposed here relies on having consistency between TRANSP simulations and neutron measurements. The methodology is based on running TRANSP without RF kick operator for cases with modulated RF power. Small corrections of the calculated neutron rates might be needed in order to match predicted fusion performance at the end of RF modulation switch off phase. In general, inconsistencies between TRANSP and measured neutrons, usually thought to be due to T_i measurement limitations and precision, should be within 10% [55], [56], [57] and in our case this is corrected by scaling the predictions to experimental data at the end of ICRH power modulation switch off period. The ratio of the measured to predicted neutrons at the end of modulated RF power on time slice then will give more robust estimate of the RF waves - fast ion interaction. This technique is now used in addition to the assessments made by predictions with and without RF kick operator, which are sensitive to the way the latter is implemented.

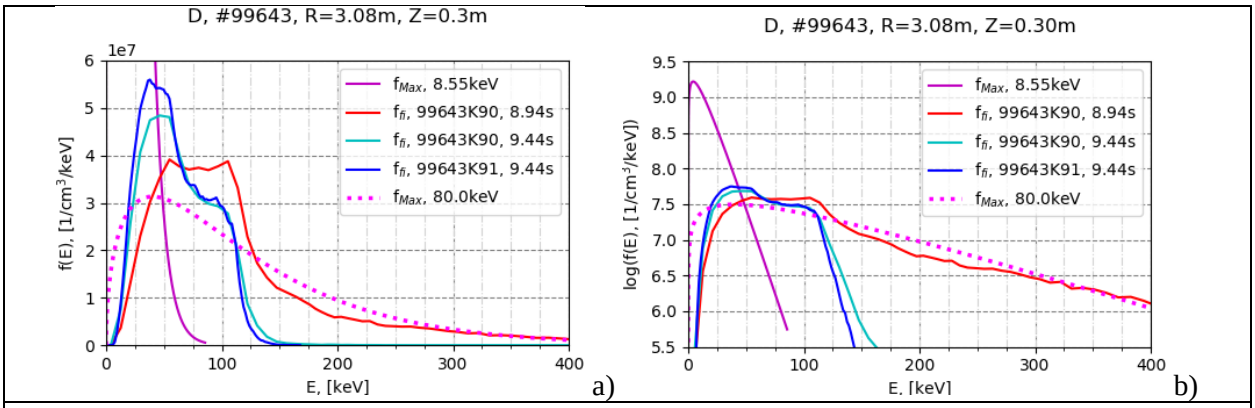

FIGURE 6. Fast ions DF $f_{fi}(E)$ for #99643 at R=3.08m, Z=0.30m in linear a) and log10 b) scale and in energy range up to 400keV. Fast ions DF at 8.94 with and P_{RF}~4MW and n_{fi}~$5.2\times10^{18}m^{-3}$ is shown in red (case 99643K90, 8.94s), while at 9.44s with P_{RF}~0.4MW and n_{fi}~$3.8\times10^{18}m^{-3}$ is shown in cyan (case 99643K90, 9.44s). The expected Fast ions DF at 8.94 with and P_{RF}~4MW and n_{fi}~$3.9\times10^{18}m^{-3}$ without taking into account RF interaction is in blue (case 99643K91, 9.44s without RF kick). For comparison shown are Maxwellian DF, f_{Max}, in magenta for n_D~$3\times10^{19}m^{-3}$, T_i=8.55keV corresponding to the D ion density and temperature at R=3.08m, Z=0.30m and energetic ion Maxwellian DF with n_{fi}~$5.2\times10^{18}m^{-3}$ and T_i=80keV in dotted magenta.

Results from the modelling and analysis of experimental data

NPA observations

JET Neutral Particle Analyzer (NPA) diagnostic can provide experimental verification of fast NBI ions interaction with RF waves. The analysis of the data from the NPA diagnostic and obtaining more quantitative assessment of the origin and the distribution of the neutrals require additional data processing and modelling of neutrals' transport in plasma. Assessing the birthplace of fast energetic neutrals from JET's NPA data is also challenging due to high densities of these pulses. In some cases, there are also non-validated NPA channels which makes the reconstruction of neutral distribution problematic. Despite all these issues qualitative observations of RF waves – fast ions interaction can be made without the need for detailed processing of the NPA data. Results from NPA analyzer are presented in figure 7 a) and b) for low energy and figure 7 c) for high energy neutrals.

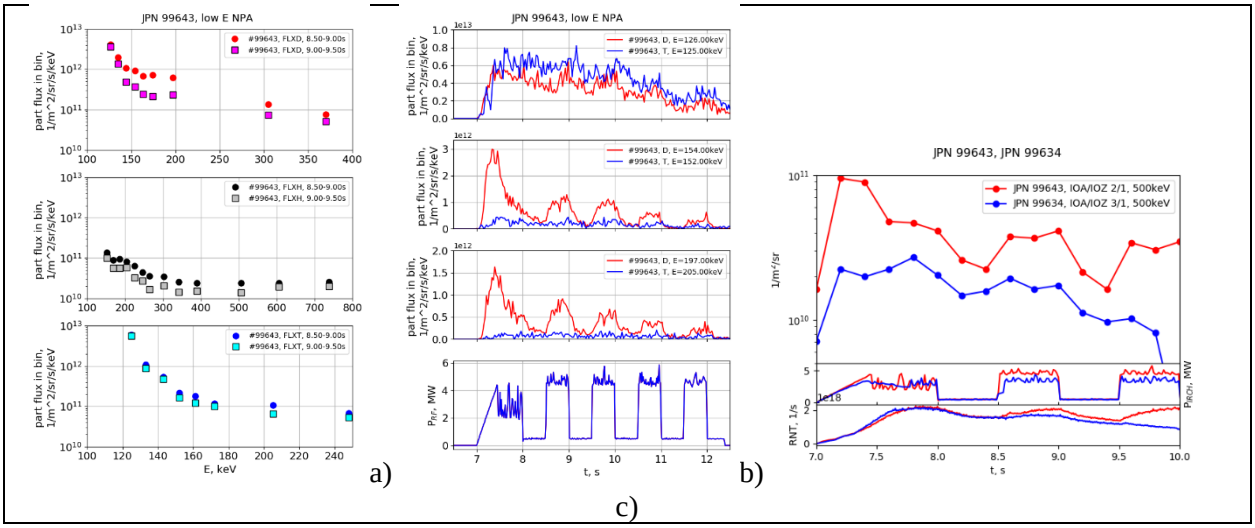

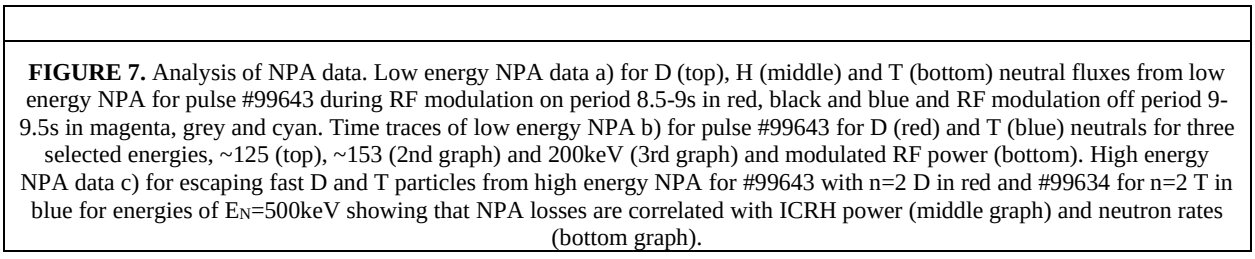

FIGURE 7. Analysis of NPA data. Low energy NPA data a) for D (top), H (middle) and T (bottom) neutral fluxes from low energy NPA for pulse #99643 during RF modulation on period 8.5-9s in red, black and blue and RF modulation off period 9-9.5s in magenta, grey and cyan. Time traces of low energy NPA b) for pulse #99643 for D (red) and T (blue) neutrals for three selected energies, ~125 (top), ~153 (2nd graph) and 200keV (3rd graph) and modulated RF power (bottom). High energy NPA data c) for escaping fast D and T particles from high energy NPA for #99643 with n=2 D in red and #99634 for n=2 T in blue for energies of E_N=500keV showing that NPA losses are correlated with ICRH power (middle graph) and neutron rates (bottom graph).

In JET conditions, central densities $n_e \approx 2n_D \approx 2n_T \approx 7\times10^{19}$ $m^{-3}$and temperatures, $T_e \approx T_i \approx 10$keV, the main collision processes acting as a source of energetic neutrals are ionizing collisions of fast ions with bulk neutrals and impurities and CX recombination between these species [50], [59]. These processes depend on background plasma parameters while escaping neutrals bear the signature, i.e. energy and pitch angle, of the fast ions they originate from. Figure 7 shows that NPA losses are correlated with RF power. Energetic D neutrals are higher during RF power on period than during RF power off period, figure 7 a). There is a small number of H neutrals which also follow this trend, while for T neutrals it seems RF power does not have an impact. The latter is clearly seen on figure 7 b) where D and T neutrals trends for selected three energies are plotted together with RF power. For energies E≈150keV to E≈200keV, D neutrals are clearly correlated with RF power while T neutrals are not. This picture is qualitatively consistent with observations in figure 4 and figure 6. Indeed, during high RF power phase energetic tail of D ions is created for energies exceeding 125keV, figure 4 b). These energetic D ion populations directly influence the source of energetic D neutrals as seen in figure 7. During low RF power phase, the energetic D ion tail disappears, figure 4 d), and so does the detected neutral D flux. Tritium is non resonant with RF wave in #99643 so T fast ion DF is unaffected and therefore detected T neutrals are not correlated with RF power. Figure 7 c) shows the correlation between RF power and D and T neutrals for highest available energy, E=500keV, for pulses #99643 with n=2 D in red and #99634 with n=2 T in blue. This is a qualitative indication that RF waves interact with fast D and T ions in plasma and accelerate ions to energies up to 500keV, which can be considered as a source for detected neutrals.

Assessment based on neutron rates and neutron camera data

Qualitatively the impact of synergistic effects on fusion performance can be assessed by analyzing the response of the DT neutron rates. The latter can be modelled or measured and achieving a good match between both provides additional confidence in the analysis. The effect of synergistic effects can be studied by modelling cases with and without RF waves – fast NBI ions interactions. Initially, this assessment was performed by means of interpretative analysis by TRANSP. Two runs of TRANSP were carried out: one with RF kick operator included in the calculations and one without it. Direct comparison between the results from these two runs gives an estimate of the impact of RF wave – fast NBI ions interaction. JETTO interpretative runs were also performed with the same input data and in a similar matter RF impact was investigated by comparing cases with realistic and negligible RF power.

Measured and calculated neutron rates together with the computed BT and thermal rates are shown in figure 8 for TRANSP simulations and figure 9 for JETTO runs. Relatively good agreement was observed between measured and calculated neutron rates with TRANSP overpredicting total neutrons at 9.0s by about 13% in #99639 and by about 8% in #99643 and underpredicting the total neutrons by about 12% in #99886. TRANSP results for plasma energy were found fully consistent, within 1%, with the diamagnetic measurements.

While measured and calculated neutrons of #99886 were higher than the ones in #99643 a closer look at the contributions to them reveal that this is due to mainly higher thermal rates. The latter is due to higher ion temperature in #99886 as it features higher NBI power. Beam-target rates of the two pulses are approximately similar despite higher NBI power of #99886.

Comparing TRANSP runs with and without synergistic effects, solid blue lines vs. dashed cyan lines in figure 8 a) and c) and solid red line vs. dashed magenta line in figure 8 b), gives TRANSP estimate of the impact of the synergistic effects on the fusion performance. The assessments provided here are all at about 9.0s. Interestingly, TRANSP predicts negligible impact of the synergistic effects on fusion performance for RF wave interaction with fast T NBI ion cases, figure 8 a) and c) blue lines and cyan dashed lines almost overlapping. There seems to be no dependence on ^{3}He minority as well since case #99639 in figure 8 a) was for X[^{3}He]≈3.6%, while case #99886 in figure 8 c) was with negligible X[^{3}He]≈0.35% i.e. pure n=2 T case. As for the RF wave interaction with fast D NBI ions, TRANSP predicts relatively reasonable improvement of fusion rates: approximately 8% for #99596 with H minority of X[H]≈2% (not shown in figure 8) raising to about 10% for #99643 pure n=2 D case with no H minorities, solid red vs. dashed magenta lines in figure 8 b).

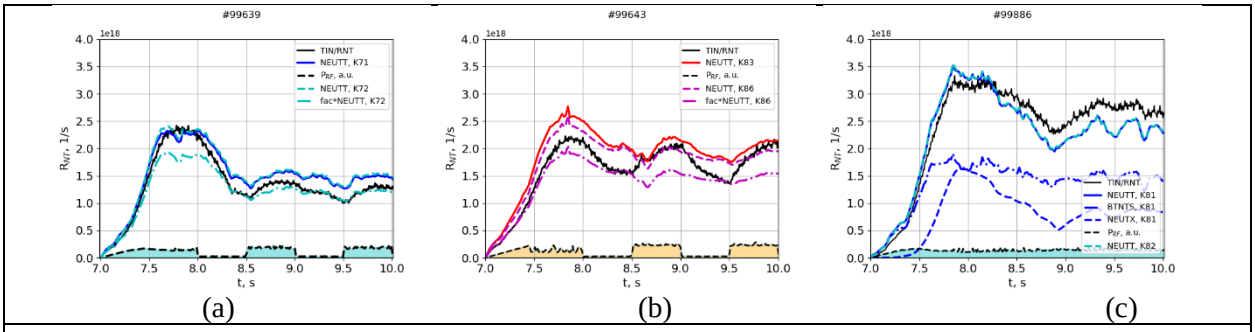

FIGURE 8. Measured, black solid lines, and calculated (blue solid line in a) for #99639 and in c) for #99886 and red solid line in b) for #99643) by TRANSP neutron rates. Beam-target reactions and thermal rates are indicated by dash-dotted blue line while thermal rates are provided by dashed blue line in c). Total neutron predictions without synergistic effects are provided by dashed-dotted cyan line in a) and c) and dashed-dotted magenta line in b). RF power time traces are provided at the bottom of each graph for illustrative purpose.

Similar type of assessment of the fusion performance enhancement due to synergistic effects was repeated with JETTO. Results of JETTO runs in which same profiles were used as with TRANSP simulations are shown in figure 9. Due to peculiarity of PION/PENCIL treatment of fast ions, synergistic effect cannot be simply switched off in JETTO. Instead, runs with full ICRH power are compared versus similar runs but with negligible RF power. This approach ensures that the thermal neutron rates are still properly accounted for in the interpretive run following T_i profile and DT mixture evolution. On the other side, RF waves – fast ion interactions have direct impact on the synergistic acceleration of fast NBI ions hence BT rates so that having negligible ICRH power in this case can be considered as removing the synergistic effect similar to switching off the kick operator in the TRANSP runs. In contrast to TRANSP predictions, JETTO predicts reasonable impact of the synergistic effects on fusion performance for RF interaction with fast T ion cases, figure 9 a) and c) blue lines and cyan dashed lines. At 9s JETTO predicts fusion enhancement due to synergistic effects of about 9% for #99639 with ^{3}He minority and about 18% for n=2 T case #99886. RF interaction with fast D ions improves the fusion rates by approximately 12% for #99596 H minority case (not shown in figure 9) and by about 29% for #99643 pure n=2 D case, solid red vs. dashed magenta lines in figure 9 b). The latter numbers are about three times higher than relevant TRANSP predictions.

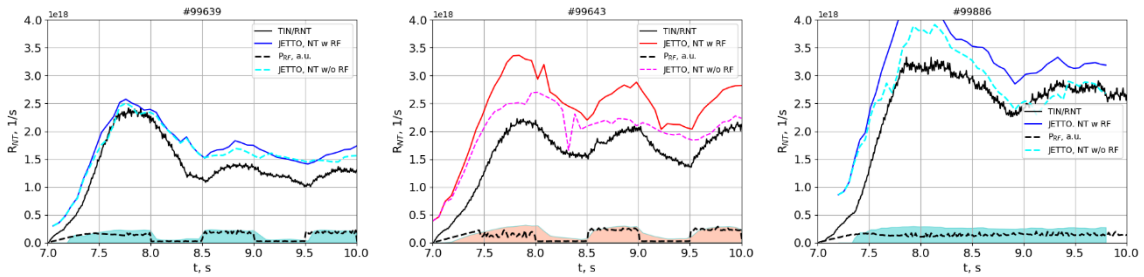

FIGURE 9. Measured (black solid lines) and calculated (blue solid line in (a) for #99639 and in (c) for #99886 and red solid line in (b) for #99643) by JETTO code neutron rates. Total neutron predictions with negligible RF power are provided by dashed cyan line in (a) and (c) and dashed magenta line in (b). RF power time traces are provided at the bottom of each graph for illustrative purpose.

Due to the observed discrepancies in TRANSP and JETTO predictions, alternative method of determining the impact of synergistic effects is discussed here. It uses the measured neutron data in pulses with modulated ICRH power and compares experimental data during periods with high RF power with TRANSP predictions without RF synergy effects. For this purpose, a number of JET pulses which featured ICRH power modulation with square waveform and low frequency of 1Hz, were analyzed. Because of the relatively longer periods with RF power being on or off, i.e. periods of 0.5s, which time duration is longer than the fast ions thermalization times, table 1 for fast D and T ions, one can assume that at the end of each ICRH power on/off period FI DF is settled and steady-state, i.e. it is non-transient and does not evolve. In addition, the ICRH power on/off periods were selected such that the background plasma parameters are not evolving and are relatively steady, as shown by the time traces in figure 3 a) and b). Consequently, by comparing fusion performance at the end of each ICRH power on/off period one can further constrain the analysis and assess the impact of the synergistic effects. TRANSP runs without RF kick operator were used again and the methodology adopted here uses the fact that TRANSP reproduces relatively well neutron rates in JET discharges [55], [56], [57]. Simulations without RF kick operator in this case are expected to match reasonably well neutron rates at the end of ICRH power off time intervals. The simulations were then compared to the experimentally measured fusion performances at the end of ICRH switch on period and the difference between modelled and measured data can be used as a more realistic assessment of the RF waves – fast NBI ions interactions. Neutron rates from TRANSP runs without RF kick operator, dashed cyan line in figure 8 a) and dashed magenta line in figure 8 b), were compared to the experimental data and scaled to match the measurements at the end of ICRH power off time, 9.5s in figure 8 a) and b). This small adjustment, usually of the order of 5-10%, of the modelled data is needed because sometimes TRANSP predictions deviate slightly from the measurements [55], [56], [57]. The scaled predictions for the computed neutron rates are then evaluated versus the measured ones at the end of RF switch on period, i.e. 9.0s in figure 8 a) and b). This procedure provides more realistic estimate of the synergistic effects and gives about 8% enhancement of the fusion performance for #99639 with n=2 T with small ^{3}He minority and about 28% for #99643 pure n=2 D case. These numbers are closer to JETTO predictions than TRANSP runs with and without RF kick operator.

The methodology described above is further applied to the measurements by the neutron camera. Channels 15 and 16 are vertical, passing in the vicinity of the plasma center and in principle should provide most accurate assessment of the line averaged rates, blue lines in figure 2 a). Time traces of neutron camera data and scaled predictions by TRANSP code are shown in figure 10. In this case TRANSP was run without RF kick and predicted neutron rates are scaled to match measurements at the end of ICRH power off phase at 9.5s. Comparing the scaled rates from TRANSP with measurements at the end of ICRH power on phase, 9s, give neutron rate enhancement of 7% for #99639 with n=2 T with small ^{3}He minority and about 25%

for #99643 pure n=2 D case. These figures are consistent with the estimates described above which are made with total neutron rate measurements and using the same procedure.

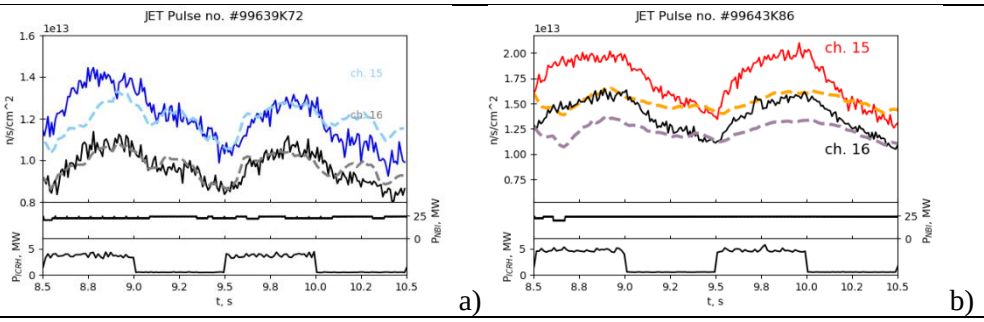

FIGURE 10. Time traces of channels 15 (blue/red solid lines) and 16 (black solid lines) from neutron camera compared to TRANSP simulations without RF kick for channels 15 (dashed orange/cyan line) and 16 (dashed gray line) for #99639 in a) and #99643 in b). NBI and RF power time traces are provided at the bottom of the graph.

MPRu analysis

Data from MPRu was available for #99886 at about 8s, i.e. pure n=2 T ICRH heating case, and relevant analysis was performed for this pulse [53]. The initial estimates were done by means of TRANSP fast ions distribution function in a workflow using an algorithm [41] which calculates expected neutron spectra, which is then converted in the expected MPRu spectrum. The latter was then compared to the MPRu measurements, i.e. data for the number of counts in scintillator detectors, figure 2 c) versus the strike position, X_{pos}, figure 2 d). Expected neutron spectrum in the MPRu LOS was calculated by means of the DRESS [41] synthetic neutron diagnostics code. For the purpose of MPRu analysis, the intensities of the calculated spectra have been rescaled to fit the data; only the shape of the spectra is validated and compared in this investigation. The results from this analysis are shown in figure 11 a)-c), where measured data for the number of counts per second registered on scattered proton position X_{pos}, black points, are plotted versus predicted MPRu spectra with FI DF from TRANSP runs without RF kick operator, dashed blue lines. Figure 11 a) shows also the calculated MPRu spectrum with FI DF from TRANSP runs RF kick operator, dashed cyan line, while the MPRu spectrum in figure 11 c) was derived with FI DF from JETTO run, dotted navy line. The spectrum noted by violet das dotted line in figure 11 b) is derived assuming FI DF from TRANSP for E<120keV and enhanced tail modelled with Maxwellian with T=80keV. The FI DFs from TRANSP used in this analysis are shown in figure 11 e)-f) correspondingly.

The predicted MPRu spectra are in decent agreement with the data from the diagnostic when TRANSP FI DFs were used, figure 11 a) and d), for scattered proton position up to $X_{pos}\approx35$cm and in poor agreement for energetic neutrons corresponding to MPRu strike positions of $X_{pos}\approx39$cm and 41cm. Very little difference between the calculated spectra by TRANSP with and without RF kick operator is predicted following the dashed blue lines in figure 11 d). Based on these two TRANSP runs with and without RF kick operator negligible impact on the fusion performance is expected to be due to RF wave – fast NBI ions interaction.

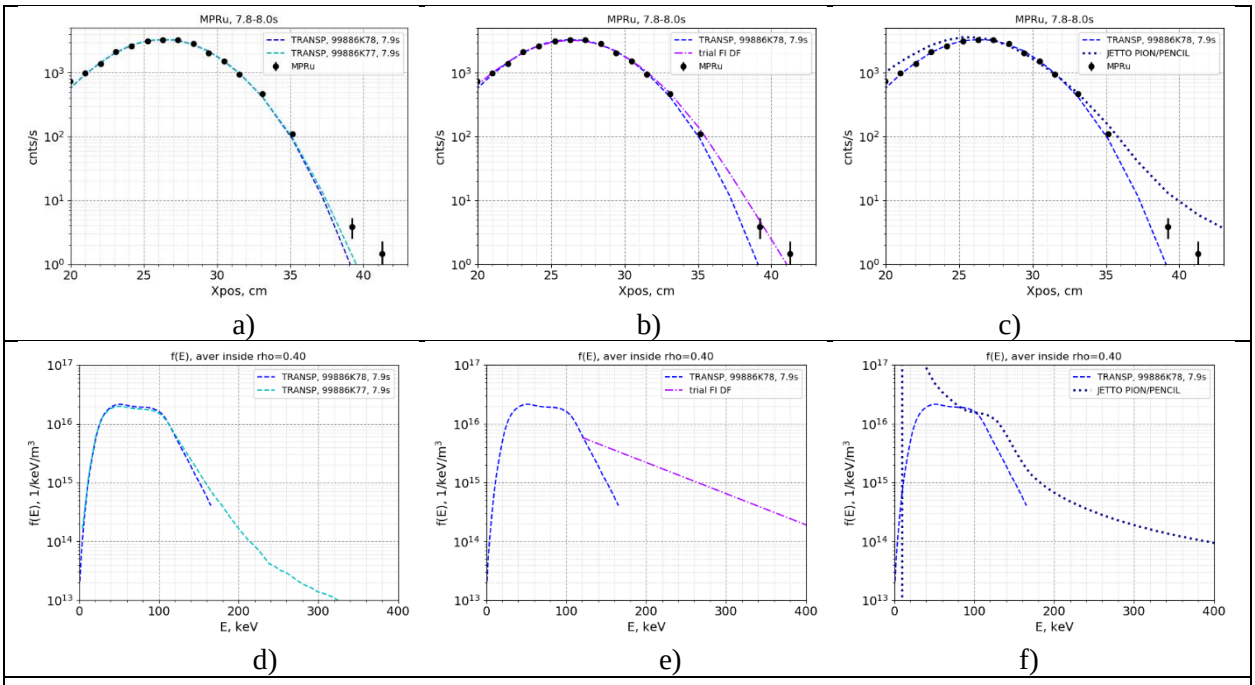

FIGURE 11. MPRu analysis for #99886. In graphs a)-c) shown are the predicted spectra using FI DF from TRANSP run 99886K78 without RF kick operator (blue dashed line) and the measured ones (black symbols). These are compared to predicted spectra using FI DF from TRANSP run 99886K77 with RF kick operator (cyan dashed line) in a), predicted spectra using FI DF from TRANSP for E<120keV and enhanced tail modelled with Maxwellian with T=80keV (violet dash-dotted line) in b) and predicted spectra from JETTO run with full RF power (navy dotted line) in c). FI DF used for calculating the spectra in a)-c) are shown in d)-f) correspondingly.

Predicted spectra with FI DF from JETTO run with full RF power are shown by dotted navy line in figure 11 c). The FI DF used in this case is presented by same style line in figure 11 f). Although this JETTO run predicted significant impact on the synergistic effects on the fusion performance, ≈18% increase, the FI DF from this JETTO run results in a spectrum which does not match MPRu measurements for X_{pos}>30cm as shown in figure 11 c). The same comparison with a trial fast T ion DF having more pronounced RF tail, violet dash dotted line in figure 11 e), has been attempted and has shown very good consistency with experimental data, figure 11 b).

The analysis based on trial fast T ion DF, having FI DF for energies up to ~120keV derived from TRANSP and more pronounced RF tail for E>120keV, figure 11 e), have demonstrated that increased RF tail in fast T ion DF leads indeed to better match of MPRu spectra, figure 11 b). This RF tail, figure 11 e) was made of Maxwellian with temperature of 80keV and is exceeding TRANSP predictions shown in dashed blue line in figure 11 e). Measured neutron spectra by MPRu seem to be very sensitive to the tail of FI DF driven by RF waves. A too low RF tail, figure 11 d) dashed blue line, leads to underestimation of high neutron energy channels, X_{pos}>39cm, while a too high RF tail produces more energetic spectra than the measurements as shown in figure 11 c) for FI DF in figure 11 f) dotted navy line. It has been assessed that the enhancement of DT fusion rate from the best fitting FI DF featuring trial RF tail with temperature of 80keV, figures 11 b) and 11 e) dash dotted violet line, is about 5%.

The results from MPRu analysis need further clarification. While FI DF with RF tail shown in blue in figure 11 e) dash dotted violet line matches very well the measured MPRu data, it is clear that this is not the only FI DF that will produce good agreement with experimental MPRu data. Undoubtedly, there are other FI DFs which will fit MPRu measurements and in general the analysis based on synthetic MPRu diagnostics should not be performed by guessing the FI DF. The FI DFs from TRANSP and JETTO however do not match the experimental data as figure 11 a), and c) show. Therefore, one naturally looks

for a possible solution which is close to the predictions by the codes. In our case this is FI DF based on predicted FI DF by TRANSP for energies up to NBI injection, E<120keV, and assuming an RF tail with temperature of 80keV for energies E>120keV, which assumption is not completely unfounded. Fast ion DFs from TRANSP are compared to Maxwellian DF with temperature of 80keV in figure 6. Clearly from figure 6 one can conclude that the latter is very good approximation for FI energetic tail for energies E>120keV.

DISCUSSION

Results from various methods used in the study to assess the impact of RF wave - fast NBI ions interaction are summarized in table 2. Column 3 gives the changes in total neutron rates, $\Delta R_{NT}/R_{NT}$, during ICRH power modulation pulses. These changes include indirect effects due to ICRH heating and therefore real enhancement of the fusion performance due to synergistic effects is expected to be lower.

TABLE 2. Estimated enhancement of DT fusion rates due to the impact of RF wave - fast NBI ions interaction. Column 3 shows the increase in total neutron rates taken at time slices at the end of RF power switch on/off in 1Hz modulation cases. Assessment a) is done using TRANSP run w/o RF kick in 1Hz modulation pulses and comparing measured neutron rates versus predicted during high RF power phase. Estimates in b) are based on similar analysis as in a) but neutron camera data from central channel 15 was used instead of total neutron rates. The enhancement noted by c) is based on MPRu analysis discussed in the previous section. Last two columns give assessment by TRANSP run with and without RF kick operator and JETTO run with very low and real RF power.

JET Pulse	scenario	ΔR_{NT} / R_{NT}, 1Hz mod	Total fusion performance enhancement due to synergy effects			
			a) ΔR_{NT} and TRANSP runs w/o RF kick	b) ΔR_{ch15} and TRANSP runs w/o RF kick c) MPRu analysis	TRANSP runs w\w/o RF kick	JETTO w\w/o RF power
#99596	H min, X[H]≈2%	N/A	**N/A**	**N/A**	**0.08**	**0.12**
#99639	^{3}He min, X[^{3}He]≈3.6%	0.20-0.30	**0.08**	**0.07** [b)]	**0.00**	**0.09**
#99643	n=2 D	0.31-0.49	**0.28**	**0.25** [b)]	**0.10**	**0.29**
#99886	n=2 T	N/A	**N/A**	**0.05** [c)]	**0.00**	**0.18**

The estimates of the synergistic effects provided in columns 4 and 5 are presently the most accurate ones as they use combinations of experimental measurements and modelling which is not dependent on the way the RF wave - fast ions interaction is implemented. The method which uses TRANSP modelling with and without RF kick operator for pure n=2 D pulse #99643 evaluates that synergistic interaction between fast NBI D ions and RF waves lead to modest improvement of the fusion performance, approximately 10% higher, table 2. On the other side, synergistic interaction between fast T NBI ions and RF waves was found to have little or no impact on the fusion performance as no increase in fusion rates has been observed in TRANSP simulations of #99639 and #99886. JETTO modelling with full and low ICRH power on the other side predicts 29% enhancement of fusion rates due to RF waves – fast D NBI ions interaction and 18% enhancement for fast T NBI ions, table 2.

Table 2 shows that TRANSP simulations with and without RF kick operator, column 6, tend to underpredict the impact of RF wave – fast NBI ions interaction on the fusion performance when compared with experimental observations by neutron diagnostics, columns 4 and 5. The RF kick operator in TRANSP attempts to capture the physics of RF wave - fast NBI ions interaction, figure 4 a) and figure 6, however, as the MPRu analysis show, figure 11 a) and d), acceleration to high energy is underpredicted. The change of FI DF in TRANSP with RF kick operator seems to be insufficient to match measured neutron spectra by MPRu.

JETTO runs with lower and realistic power, table 2 column 7, seem to overpredict the enhancement of fusion performance for the case #99886 with n=2 T without minorities. Fast ion DF by PION/PENCIL in this case, figure 11 f), seem to be overestimating the extent of RF tail particularly in high-energy end as it results in a poor fit to MPRu data, figure 11 c). JETTO predictions are however in a relatively good

agreement with the assessments from neuron measurements and TRANSP modelling without RF kick operator, columns 4 and 5, for the cases with modulated RF power, i.e. #99643 with n=2 D without minorities and #99639 with X[^{3}He] ≈ 3.6%.

Neither of the two methods based on numerical analysis with and without RF wave – fast ions interaction appear to be capable to predict very accurately the enhancement of the fusion performance. The reason for the significant differences in these predictions could be in the way the RF wave – fast ions interaction is implemented in TRANSP and JETTO. Both codes use various simplifications and approximations to the RF kick operator and RF induced quasi-linear diffusion, which could eventually result in TRANSP underpredicting and JETTO overpredicting the FI DF energetic tail as indicated by MPRu analysis. Simplification of fast ion orbit effects in PION/PENCIL should not be a large contribution factor as fast D and T NBI ions in these experiments are only expected to deviate only few cm from flux surface.

According to the results from TRANSP and JETTO impact of RF wave – fast NBI ion interaction decreases when adding minorities even at low concentrations, X[H, ^{3}He] ≈ 2-4%. The methods of analysis based on MPRu and ΔR of neutron data, columns 4 and 5 in table 2, show a little or even positive effect on fusion performance by adding small amount of X[^{3}He] ≈ 3-4% in n=2 fast T NBI interaction, #99886 vs. #99639. In general, adding negligible amount of minorities should help with regard to generating more favorable E_+ electric field near ion cyclotron resonance. Adding too high minority concentration, e.g. X[^{3}He] ≥ 1%, however would result in most of the RF wave power being absorbed by the minorities and lower amount of it available for interaction with fast ions. The two methods of analysis however, MPRu and ΔR of neutron data, have different source of errors and for more complete conclusions on the impact of the minorities one would ideally want to analyze #99886 n=2 T case with modulated RF power, or #99639 with ^{3}He minority by means of MPRu. Unfortunately, this kind of analysis and comparisons were not possible during JET DTE2 campaign.

Both modelling approaches as well as the data based on experimental observations indicate that accelerating fast D NBI ions by means of interaction with RF waves was more beneficial with regard to the fusion rates than accelerating fast T NBI ions. This conclusion seems to be counter intuitive, given the cross-sections for the two cases presented in figure 1. Indeed, one would expect that accelerating fast T NBI ions from NBI energy range E_T≈40-120keV to energies exceeding 200keV would benefit significantly BT fusion rates. Nevertheless, it seems better enhancement has been observed when RF waves interact with fast D NBI ions. One possible reason for this is that T beam penetration is not as central as D beams. Indeed, for D and T beams at the same energy the latter will have lower velocity by factor of 0.81 due its higher mass. This means that when both are used in same target plasma, neutral T beams will travel shorter distance before being ionized. For plasma optimized for central D NBI deposition it would mean that T deposition would be further away off axis. The latter is illustrated in figure 12 where fast D in a) and T in b) ion densities are plotted for #99886 at 9.4s. Clearly, fast D density is higher in the center, while fast T ion density is highly asymmetrical azimuthally shifted towards outboard. Another reason for observed lower fusion enhancement in T NBI case is due to unfavorable resonance location in this case which is shifted to the LFS, ~0.15m, away from the plasma center, cf. figure 4 a) with figure 12 b). The combination of all these factors would result in having lower number of T fast ions to interact with RF waves in the vicinity of the resonance, hence lower strength of the synergistic effects. It is also worth noting that BT reactivity for fast D NBI ions has slightly higher maximum and is greater than fast T NBI BT reactivity for up to energies of 165keV, figure 1. RF waves can accelerate fast NBI ions up to energies of few hundreds of keV, but it also changes FI DF for lower energies, in the domain where D NBI BT reactivity is greater i.e. E_D≈21-165keV, figure 1 and figure 6, and it seems that ions in this energy range have greater contribution to BT reactions.

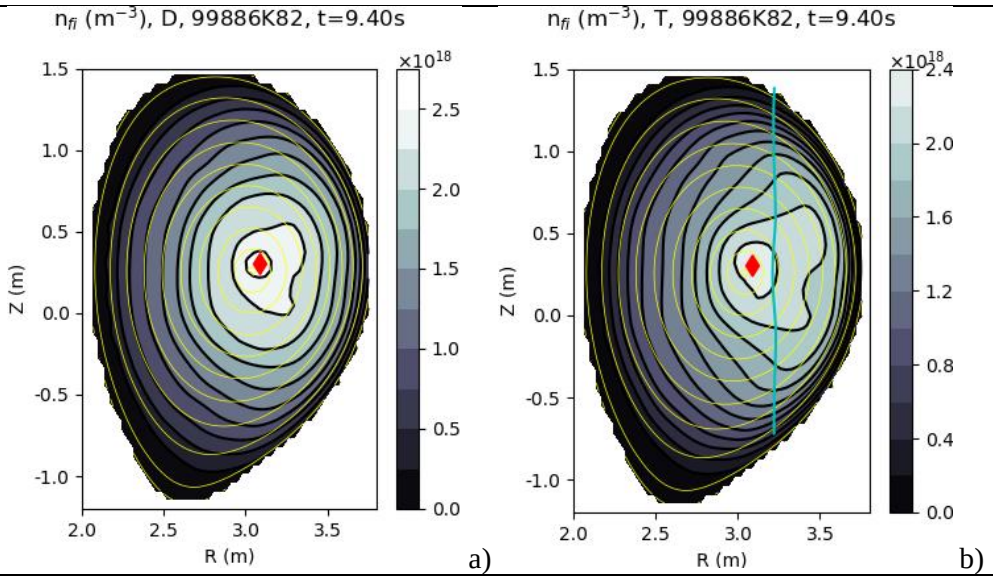

FIGURE 12. Fast D in a) and T in b) NBI ion density from TRANSP code for case 99886K82 at 9.4s. Cold plasma n=2 T resonance is indicated in b) by cyan line.

CONCLUSIONS

TRANSP and JETTO simulations were used to study the impact of the synergistic effects between fast D and T NBI ions and RF waves on DT fusion performance. The modelling results were validated versus synthetic diagnostics.

The figures based on the experimental data indicate approximately 25% enhancement of fusion rates due to RF interaction with fast D NBI ions and approximately 5-8% when RF wave – fast T NBI ions interaction is taking place. TRANSP underpredicts the improvement of fusion rates, while JETTO overpredicts them. Based on conclusions in this study, much more detailed and in-depth analysis would be needed to understand how the algorithms on RF wave – fast ions interaction are working in each case. The results here suggest that such a further study is necessary in order to understand and highlight possible improvements to the models in the future.

All methods of assessment indicate that regarding the fusion performance it is more beneficial to consider RF wave – fast D NBI ions interaction for the JET NBI energy ranges and plasma conditions. A plausible explanation of this phenomenon could be in the shallower penetration of T beams when compared to more central D beams. As a result of this study, we conclude that the scenario with fast T NBI ions can be further optimized with respect to achieving higher fusion performance.

Planned JET DTE3 campaign would not have T NBI source so studying the RF wave – fast T NBI ions interaction and in particular by means of application of modulated RF power would not be possible. This on the other side would be a great opportunity to study RF wave – bulk T ions. Application of modulated power is again strongly advisable in order to have a better assessment of the synergistic effects.

ACKNOWLEDGMENTS

This work has been carried out within the framework of the EUROfusion Consortium, funded by the European Union via the Euratom Research and Training Programme (Grant Agreement No 101052200 — EUROfusion) and from the EPSRC [grant number EP/W006839/1]. To obtain further information on the data and models underlying this paper please contact PublicationsManager@ukaea.uk . Views and opinions expressed are however those of the author(s) only and do not necessarily reflect those of the European

Union or the European Commission. Neither the European Union nor the European Commission can be held responsible for them.

REFERENCES

1. M. Kikuchi, K. Lackner, M. Q. Tran, Fusion Physics, IAEA, Vienna (2012), https://www-pub.iaea.org/MTCD/publications/PDF/Pub1562_web.pdf
2. M. Schneider et al, Nucl. Fusion 61 126058 (2021)
3. A. J. Creely et al, Overview of the SPARC tokamak, J Plas Phys, vol 86, 865860502 (2020)
4. R. V. Budny et al, Nucl Fusion 52 023023 (2012)
5. Ye. O. Kazakov et al Physics of Plasmas 28, 020501 (2021)
6. Ye. O. Kazakov et al "Applications of Three-Ion ICRF Heating for ITER", Theory of Fusion Plasmas Joint Varenna - Lausanne International Wworkshop, Villa Monastero, Varenna, Italy (2016)
7. ITER Physics Basis Editors, Nucl. Fusion 39 2137 (1999)
8. M. Shimada et al, Nucl.Fusion 47 S1 (2007)
9. R. V. Budny, M. Gorelenkova, 57th Annual Meeting of the APS Division of Plasma Physics, Volume 60, Number 19, GP12.00127 (Savannah, Georgia, 16–20 Nov 2015) (2015)
10. D. F. H. Start et al, Nucl. Fusion 39 321 (1999)
11. K. K. Kirov et al Nucl Fusion 59 056005 (2019)
12. E. Lerche et al Plasma Phys. Control. Fusion 51 044006 (2009)
13. D. Gallart et al, Nucl.Fusion 58 106037 (2018)
14. J. M. Noterdaeme et al Fusion Energy 1998 (Proc. 17th Int. Conf. Yokohama, 1998) (Vienna: IAEA) CD-ROM file and http://www.iaea.org/programmes/ripc/physics/start.htm (1998)
15. A.M. Messiaen etal Plasma Phys. Control. Fusion 35 A15 (1993)
16. M. J. Mantsinen et al Nucl. Fusion 44 33 (2004)
17. D. van Eester et al Plasma Phys. Control. Fusion 51 044007 (2009)
18. M. Schneider et al Nucl. Fusion 56 112022 (2016)
19. H. Henriksson et al Nucl. Fusion 46 244 (2006)
20. H. Kimura et al Nucl. Fusion 31 83 (1991)
21. R. Bilato et al Nucl. Fusion 51 103034 (2011)
22. J. Wesson, Tokamaks, 4th edn Oxford, Oxford University Press (2011)
23. T.H. Stix, Plasma Phys. 14 367 (1972)
24. R.J. Goldston et al, Journal Comp Physics 43 61 (1981)
25. K. K. Kirov et al RF Conf (2022), AIP conf proc (2023)
26. R. J. Hawryluk et al "An Empirical Approach to Tokamak Transport", in Physics of Plasmas Close to Thermonuclear Conditions, ed. by B. Coppi, et al., (CEC, Brussels, 1980), Vol. 1, pp. 19-46
27. A. Pankin, D. McCune, R. Andre et al., "The Tokamak Monte Carlo Fast Ion Module NUBEAM in the National Transport Code Collaboration Library", Computer Physics Communications Vol. 159, No. 3 (2004) 157-184.
28. M. Brambilla, Plasma Phys. Control. Fusion 41, 1 (1999)
29. Hammett G.W. Fast ion studies of ion cyclotron heating in the PLT tokamak PhD Thesis Princeton (1986)
30. Kwon J.-M. et al. Bull. Am. Phys. Society (2006), http://meetings.aps.org/link/ BAPS.2006.DPP.VP1.115
31. Kwon J.-M., McCune D. and Chang C.S. 2007, Bulletin of the American Physical Society 49th Meeting of the Division of Plasma Physics (Orlando, FL) (http://meetings.aps.org/link/BAPS.2007.DPP.UP8.83)
32. T. H. Stix, Nucl. Fusion 15 737 (1975)
33. C. F. Kennel, F. Engelmann, Phys Fluids, vol 9, 2377 (1966)

34. M. Romanelli et al, Plasma and Fusion Research 9 3403023 (2014)
35. L-G. Eriksson et al, Nucl. Fusion 33, 1037 (1993)
36. M. J. Mantsinen et al Plasma Phys. Control. Fusion 41 843 (1999)
37. P. Stubberfield and M. Watkins, JET-DPA(06)/87 (1987)
38. C. D. Challis 1989, Nucl. Fusion 29, 563 (1989)
39. J. Hobirk et al subm. Nucl. Fusion, Special Issue (2023)
40. H.S. Bosch, G.M. Hale Nucl.Fusion 32 611 (1992)
41. J. Eriksson et al Comp. Phys. Comm 199 40-46 (2016)
42. C. Gowers et al Rev. Sci. Instrum. 66 471 (1995)
43. E. de la Luna et al Rev. Sci. Instrum. 74 1414 (2001)
44. L.C. Ingesson, Comparison of methods to determine the total radiated power in JET, JET Report JET-R(99)06 (1999)
45. T.M. Biewer et al, “Charge Exchange Recombination Spectroscopy Measurements from Multiple Ion Species on JET”, JET report EFDA–JET–CP(07)03/24 (2007)
46. V. Zoita et al., "Neutron fluence measurements on the JET tokamak by means of super-heated fluid detectors," 2009 IEEE International Conference on Plasma Science - Abstracts, San Diego, CA, 2009, pp. 1-1, doi: 10.1109/PLASMA.2009.5227402 (2009)
47. J.M. Adams, Nuclear Instruments and Methods in Physics Research A329 (1993) 277-290 (1993)
48. G. Ericsson et al, Rev. Sci. Instrum., 72, 759 (2001)
49. E. Andersson Sundén et al, Nucl. Instrum. Methods. A, 610, 682 (2009)
50. A.A. Korotkov et al Nucl. Fusion 37 35 (1997)
51. C. Challis et al, 48th EPS Conference on Plasma Physics, 27 June - 1 July 2022
52. E.Lerche et al., Fundamental ICRF heating of Deuterium ions in JET-DTE2, in Proc. of 24th Topical Conference on Radio-frequency Power in Plasmas, Annapolis, Maryland (USA), September 2022
53. M. Mantsinen et al subm. Nucl. Fusion, Special Issue (2023)
54. P. Mantica et al subm. Nucl. Fusion, Special Issue (2023)
55. Z. Stancar et al Nucl. Fusion 61 126030 (2021)
56. K. Kirov et al Nucl Fusion 61 046017 (2021)
57. Z. Stancar, K. Kirov et al subm. to Nucl. Fusion (2023)
58. H. Weisen et al Nucl. Fusion 57 076029 (2017)
59. I. H. Hutchinson, Principles of Plasma Diagnostics, Cambridge University Press, (2002)